IOPscience iopscience.iop.org

Home Search Collections Journals About Contact us My IOPscience

Free-form design of rotor blades

This content has been downloaded from IOPscience. Please scroll down to see the full text.

2014 J. Phys.: Conf. Ser. 524 012041

(http://iopscience.iop.org/1742-6596/524/1/012041)

View the table of contents for this issue, or go to the journal homepage for more

Download details:

IP Address: 131.175.12.9
This content was downloaded on 30/03/2017 at 12:53

Please note that terms and conditions apply.

You may also be interested in:

Airfoil design: Finding the balance between design lift and structural stiffness
Christian Bak, Nicholas Gaudern, Frederik Zahle et al.

Characterization and Control of Unsteady Aerodynamics on Wind Turbine Aerofoils
J Naughton, J Strike, M Hind et al.

Design of a family of new advanced airfoils for low wind class turbines
Francesco Grasso

Design, manufacturing and characterization of aero-elastically scaled wind turbine blades for testing active and passive load alleviation techniques within a ABL wind tunnel
Filippo Campagnolo, Carlo L Bottasso and Paolo Bettini

Investigation and Optimization of Blade Tip Winglets Using an Implicit Free Wake Vortex Method
Stephen Lawton and Curran Crawford

Numerical Studies on a Rotor with Distributed Suction for Noise Reduction
Thorsten Lutz, Benjamin Arnold, Alexander Wolf et al.

Development of a Wind Turbine Test Rig and Rotor for Trailing Edge Flap Investigation: Static Flap Angles Case
Ahmed Abdelrahman and David A Johnson

Investigation of the effect of bending twisting coupling on the loads in wind turbines with superelement blade definition
M O Gözcü and A Kayran

Free-form design of rotor blades

CL Bottasso[1,2], A Croce[2], L Sartori[2] and F Grasso[3]

[1] Wind Energy Institute, Technische Universität München, Garching, Germany
[2] Dipartimento di Scienze e Tecnologie Aerospaziali, Politecnico di Milano, Milano, Italy
[3] Energy Research Centre of the Netherlands, Petten, The Netherlands

E-mail: carlo.bottasso@tum.de

Abstract.
This work investigates an integrated free-form approach for the design of rotor blades, where airfoil shapes are treated as unknowns. This leads to the simultaneous optimization of the chord, twist and structural design variables, together with the airfoil shapes along the blade. As airfoils are automatically tailored to the evolution of the blade, this process results in a better exploration of the solution space and relieves the user from the burden of up-front choices, leading to better final designs. The proposed approach is demonstrated by sizing a 2 MW wind turbine blade.

1. Introduction

The design of rotor blades for wind turbines is a highly multi-disciplinary activity, which involves the determination of the aerodynamic shape of the blade, the choice of materials and the sizing of all structural members. The design must satisfy a large number of constraints, which account for various aspects of the problem such as noise, structural integrity, manufacturability and transportability. A typical design strategy is based on the minimization of the cost of energy, with the simultaneous satisfaction of all constraints, and could be summarized by the following iterative process:

- a collection of existing suitable airfoils is selected;
- the blade chord, twist, pre-bend/cone and possibly sweep are defined;
- materials are chosen and the blade structural members are sized.

Several iterations are conducted among these design steps, until all constraints are satisfied and an optimal configuration has been achieved.

Although this procedure is commonly employed by industry, it is inherently limited in the exploration of the design space to a set of pre-assumed airfoils. It must be noticed that the shape of the various airfoils influences not only the aerodynamic performance of the blade, but also its structural sizing. In fact, cross-couplings of the aerodynamic shape on the structure affect thickness distributions of the various structural members, as well as stiffness, mass and inertia distributions along the blade span. In turn, all aerodynamic and structural parameters influence the cost of energy, so that the effect of the airfoil design is not limited to the aerodynamic performance of the blade but, on the contrary, plays a crucial role in the overall design and efficiency of the wind turbine. As a consequence, the fact that airfoils are considered as frozen throughout the blade design process, somewhat hinders a full exploration of the design space.


Content from this work may be used under the terms of the Creative Commons Attribution 3.0 licence. Any further distribution of this work must maintain attribution to the author(s) and the title of the work, journal citation and DOI.
Published under licence by IOP Publishing Ltd

To overcome such limitations, the present work describes an integrated aero-structural approach that aims at a real free-form optimization of rotor blades. Objective of the work is the definition of a new blade design procedure, whereby airfoils are designed *together* with the rest of the blade, resulting in a more complete exploration of the design space. Another scope of this new procedure is to relieve the designer from a priori choices: since the optimization process can operate directly on the airfoil shape, the importance of a proper choice in the initial set of airfoils is significantly reduced, and actually altogether eliminated. Specifically, as the airfoil design is automatically tailored to the rest of the blade, the proposed free-form approach ensures the natural emergence of typical configurations as for example flatback airfoils, automatically and without a priori assumptions, if such shapes represent optimal choices in certain parts of the blade. Additionally, airfoils at different span locations are free to adapt to different local conditions, which depend on the relative importance of the aerodynamic and structural requirements at that location. The idea of simultaneously designing airfoils and rotor was previously described in [1], although limitedly to the sole aerodynamic optimization of the blade; that idea is here generalized to the complete aero-structural design problem.

2. Free-form design of rotor blades

2.1. Optimization problem

In this work, the aero-structural design of a rotor blade is expressed as a single-objective constrained optimization problem. The cost function is based on the cost of energy to capture the tradeoffs between aerodynamic and structural efficiencies, while constraints are used to express desired features in the solution, including the satisfaction of international certification guidelines [2, 3]. The optimization problem can be formulated as follows:

$$\min_{\boldsymbol{p}} J(\boldsymbol{p}), \tag{1a}$$

$$\text{s.t.: } \boldsymbol{p}_{\min} \leq \boldsymbol{p} \leq \boldsymbol{p}_{\max}, \tag{1b}$$

$$\boldsymbol{g}(\boldsymbol{p}) \leq 0, \tag{1c}$$

$$\boldsymbol{h}(\boldsymbol{p}) = 0, \tag{1d}$$

where $J(\boldsymbol{p})$ is the objective function, $\boldsymbol{p}$ the vector of the n design variables, whose lower and upper bounds are expressed by Eqs. (1b), while Eqs. (1c) and (1d) are, respectively, the inequality and equality constraints.

The numerical solution of problem (1) is here obtained by the sequential quadratic programming (SQP) algorithm, in the implementation of [4], with slight modifications that allow for a parallel and optimized evaluation of the gradients.

The optimization procedure is based on the monolithic solution of problem (1), where the aerodynamic and structural design variables are computed simultaneously. At each iteration, the logical steps in the computation of cost function and constraints can be summarized as follows:

(i) At first, the two-dimensional aerodynamic properties of the airfoils are estimated. In traditional optimization procedures, this step is performed once at the beginning of the process, when wind-tunnel or numerical data are provided for a chosen set of airfoils. Quite to the contrary, in the free-form approach airfoils are continuously updated during design and this requires that the coefficients of lift C_L, drag C_D and moment C_M are computed numerically at each iteration. At this stage, the relevant design unknowns are represented by the shapes of the different airfoils, which are parameterized using Bézier curves (see § 3.1).

(ii) Next, the aerodynamic characteristics of the rotor are computed by a classical blade element momentum (BEM) approach (see § 3.2). The analysis computes all operating conditions

that are necessary to define the regulation trajectory of the machine and its annual energy production (AEP), including the maximum power coefficient, C_P^*, and its corresponding tip speed ratio (TSR), noted λ^*. Here, the relevant design unknowns are represented by the Bézier control points of the chord and the twist spanwise distributions.

(iii) Next, a structural analysis follows to determine all relevant properties, including sectional mass, inertias and stiffnesses. This allows one to define a complete beam model of the blade, which in turn enables the computation of the lower eigenfrequencies (here limitedly to the first flap mode) and the simulation of all relevant design load cases (DLC) (here limitedly to a set of storm conditions similar to DLC 6.2 [3]). In this case, the relevant unknowns are represented by the thicknesses of the spar caps (assumed equal on the blade suction and pressure sides) while, for simplicity, other structural elements as the shell and the shear webs are here considered as frozen. By post-processing the results of the DLCs, the conditions of maximum tip deflection and maximum stress/strain at all cross sections of interest are readily identified, and used for the evaluation of the associated inequality constraints.

(iv) Finally, the cost of energy (CoE) is calculated following [5]. If an optimal solution that satisfies all constraints has been reached, the optimization is halted, otherwise a new iteration is initiated and the cycle is repeated until convergence.

It should be pointed out that sub-problems 1 to 3 are intimately coupled to one another. As the local thickness of the airfoils is changed during optimization, the structural properties of the blade are also affected. This could happen at a local level (stress/strain, thickness of the elements), or at a global one (blade mass, frequencies). On the other hand, the shape of each airfoil has also implications on the local lift, drag and efficiency, which in turn affect the loading and the overall power production of the rotor. As a consequence, the airfoil design is also coupled to the evolution of the blade chord and twist. Therefore, as mentioned in the introduction, the ability to design the airfoils together with the rest of the blade implies couplings and cross-effects that go well beyond the pure two-dimensional aerodynamic characteristics of the blade sections.

2.2. Objective function and constraints

The ability to carry out a true multi-disciplinary design must rely on appropriate models, which should be able to effectively summarize the performance of the blade, and must capture all relevant aspects of the design. For what concerns the choice of the objective function, a good strategy is to pursue the minimization of the CoE, as illustrated in [6]. In this work, the objective function is based on the cost model developed at NREL [5], which expresses the CoE as follows:

$$\mathrm{CoE} = \frac{\mathrm{FCR} \cdot \mathrm{ICC}(\boldsymbol{p})}{\mathrm{AEP}(\boldsymbol{p})} + \mathrm{AOE}(\boldsymbol{p}), \tag{2}$$

where FCR is the fixed charge rate, ICC the initial capital cost, and AOE the annual operating expenses.

In principle, this physics-based cost model allows one to draw a direct link between design parameters and cost of energy. For example, by the knowledge of the blade geometry and constituents, one may derive a complete bill of materials and hence the blade material cost may be computed. Similarly, from the rotor torque one may estimate the gear-box mass and hence cost, by using a suitable physical sub-model or scaling relationships based on historical data. All of these quantities, mass and cost of blades and gear-box, would contribute to the ICC in Eq. (2); similar examples could be made for all main components of the machine. By the same token, the aerodynamic parameters describing airfoils, chord and twist distributions influence directly the AEP, but also affect the loads, which in turn feed into both the ICC and AOE in Eq. (2).

The design constraints should reflect all desired characteristic of the solution, as explained in [7, 8], including performance, safe operation in all conditions encountered throughout the lifetime of the machine, fatigue, aeroelastic stability, manufacturing constraints, transportation and assembly, etc. In general, the bulk of such conditions are described by international design standards [2, 3], and complemented by the designer in order to express all desired and necessary features of the solution.

To make an initial assessment of the free-form approach proposed here, and to prove the concept, only a limited set of such conditions was considered in this work. Such subset was selected in order to be simple and not excessively expensive to compute, but at the same time reasonably complete so as to lead to realistic blade solutions.

In particular, the monolithic approach expressed by equations (1) implies that both the aerodynamic and structural design variables are solved simultaneously. If an extensive set of DLCs is used, their re-computation for each change in each design variable dominates the computational cost and rapidly leads to very expensive problems. To curb this effect, the dynamic DLCs were here limited to one single set of storm conditions, as these often (although not always and not on all components) generate ultimate loads on wind turbines. For a similar reason, fatigue was not included in the structural design.

Furthermore, the adoption of the SQP method for the solution of algorithm (1) necessitates of a smooth cost function as well as of smooth constraints, since the algorithm is driven by gradient information. In case an extensive set of DLCs is considered, it may happen that ultimate loads suddenly jump from one DLC to another even for small changes in the design variables, leading to a loss of smoothness that may preclude the solution via a gradient-based method.

It should be stressed that both issues described above, i.e. computational cost and possible lack of smoothness, are not specific to the free-form approach, but are general characteristics of the aero-structural design of wind turbines. Both issues can be addressed by suitable reformulations of the design problem and by proper choices of the numerical solution algorithms, which however go beyond the scope of the present work.

To address the above concerns, and still have a reasonable set of design constraints, the following were considered in this work:

- Resonance avoidance. This constraint affects the first flap blade frequency f_{flap}, which is required to be higher than the three-per-revolution harmonic f_{3P}. This condition can be expressed as:
$$g_f = \epsilon_{\text{freq}} - \frac{f_{\text{flap}}}{f_{3P}} \leq 0, \tag{3}$$
where ϵ_{freq} is the desired relative clearance between the two. This constraint, posing a lower limit on the first flapwise frequency of the blade, avoids resonance and hence vibrations. Since the first flapwise frequency depends largely on the out-of-plane stiffness of the blade, this constraint regulates the thickness of the airfoils and the sizing of the structural elements, and specifically of the spar caps.
- Stress verification. At each section, stresses are enforced to be lower than the allowables in order to ensure that the blade can withstand ultimate loads, which in the present case are assumed to derive from storm conditions. This design constraint can be expressed by the relation:
$$g_\sigma = \epsilon_\sigma - \frac{\sigma_{\text{adm}}}{\sigma_{\max}} \leq 0, \tag{4}$$
where $\sigma_{\max}$ is the maximum stress detected in each element, σ_{adm} the allowable stress and ϵ_σ a tolerance that has the meaning of a safety factor.

Other simple geometric constraints may be considered, as necessary, to limit the maximum chord (for example, to express a transportability condition), or to limit the spanwise rate of

change of the thickness of structural elements (for example, to translate technological and/or manufacturing constraints).

3. Mathematical models

3.1. Two-dimensional aerodynamics

The core feature of the free-form method is that the airfoil shapes are allowed to change during the blade design process. While in the traditional optimization approach aerodynamic data for the airfoils is supplied once and for all through look-up tables, here airfoil aerodynamics must be described by an appropriate model and updated at each iteration.

In this work, airfoils are defined at selected stations along the blade span. At each one of these stations, the shape of the local airfoil is parameterized using assumed bases, and its two-dimensional characteristics are computed. Then, as routinely done in blade analysis, the shape and aerodynamic characteristics at other stations are obtained by spanwise interpolation.

Following [9], the geometry of each airfoil is parameterized using Bézier curves [10], so that the two-dimensional coordinates $\boldsymbol{x}$ of each point are readily expressed in terms of the coordinates $\boldsymbol{x}_{\mathrm{cp}}$ of a number of control points, i.e. $\boldsymbol{x} = \boldsymbol{x}(\boldsymbol{x}_{\mathrm{cp}})$. Two distinct control points are used at the trailing edge, so that flatback airfoils can be readily represented by the assumed parameterization. It was found that four third-order Bézier curves are typically sufficient in order to generate a very wide variety of typical airfoil shapes; the four curves are arranged in order to assure geometric continuity between two contiguous arcs, so that each airfoil is eventually defined by 13 control points, as shown in Figure 1.

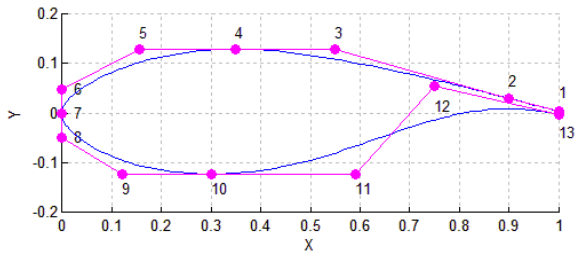

Figure 1. Airfoil parameterization using Bézier curves, including control points (dots) and resulting airfoil shape (blue solid line).

Given its geometry, as parameterized above, the aerodynamic characteristics of each airfoil are evaluated numerically with the method of [11, 12], as implemented in the `Xfoil` code. This inviscid formulation is based on a linear-vorticity stream function panel method, with the addition of a Karman-Tsien correction in order to take into account the effects of compressibility. The viscous analysis relies on a two-equation lagged dissipation integral boundary layer formulation, which is coupled with the inviscid solution through a surface transpiration model. The analysis is performed in the range of angles ± 20 deg; the resulting curves are then extended to the full range ± 180 deg by means of the Viterna method [13]. The two-dimensional analysis is repeated for different Reynolds numbers (here, typically two), in order to cover the range of operating conditions of interest of each airfoil.

3.2. Three-dimensional aerodynamics

The aerodynamic modeling of the rotor is based on a classical BEM approach [14]. The blade is described along a spanwise non-dimensional coordinate $\eta \in [0, 1]$ in terms of its local chord length, aerodynamic twist, position of the aerodynamic center and in terms of the tabulated

airfoil characteristics obtained numerically as explained above. Chord and twist distributions are parameterized by using Bézier curves, which allow for a significant freedom in the description of rotor blade shapes. Intermediate airfoils, at stations other than the airfoil design ones, are obtained by interpolation, so that the absolute thickness can vary smoothly along the entire blade length. Specific airfoils can be frozen, if necessary; for example, cylinders and transitional airfoils close to the blade root are usually kept unchanged throughout the optimization. For this reason, each airfoil can be listed as active, if it participates in the optimization, or not.

The evaluation of the aerodynamic performance of the rotor is based on the methodology outlined in [7], and starts with a BEM analysis for the determination of the power coefficient $C_P = C_P(\lambda, \beta)$ as a function of TSR λ and blade pitch β, assuming an exponential vertical wind shear. The correction of Prandtl is used in order to take into account tip-losses, as indicated in [15], and hub-losses are modeled as well. From the computed C_P-λ-β curves, the regulation trajectory of the machine is obtained following [16]. The formulation computes the power curve by taking into account the presence of region II (partial power, constant TSR strategy) and III (full power strategy). In the presence of limits on the maximum tip speed or the rotor speed, an additional transition region $II^1/_2$ is generated between the two. This requires to solve, for each value of the wind speed V in the range $[V_{II^1/_2}, V_r]$ the following optimization problem [16]:

$$C_P^{II^1/_2}(V) = \max_{\beta} C_P(\lambda(V), \beta), \tag{5a}$$

$$\beta^{II^1/_2}(V) = \arg\max_{\beta} C_P(\lambda(V), \beta). \tag{5b}$$

Alternatively, one may reduce TSR in the transition region by keeping the blade pitch setting constant, at the price of a small reduction in power coefficient.

Once the power curve has been obtained, the AEP is computed by multiplying the power curve with an appropriate Weibull distribution, which accounts for the statistical occurrence of the different wind speeds at the installation site.

3.3. Structural beam and cross-sectional models

The blade is modeled as an Euler-Bernoulli beam [17]. Transverse shear is neglected while warping, although not explicitly accounted for, could be recovered by the torsional behavior of the blade. The beam model is discretized using a finite element formulation featuring 15 degrees of freedom per element, of which 3 model torsion and 4 each are used for axial, flap, and lag deflections. The beam model, which includes Coriolis and centrifugal stiffening effects, is described in terms of the spanwise distributions of flap, lag, torsional and axial stiffnesses, mass, section moments of inertia, chordwise offsets of the shear center, tension center, and center-of-mass at each section along the blade.

The internal configuration is assumed to be a three-cell box section whose structural elements include an external shell, two spar caps and two shear webs, as shown in Figure 2, at left. The spar cap thicknesses are assumed as design variables, and are discretized along the spanwise coordinate using Bézier curves; the same thickness is assumed for the suction and pressure sides of the blade.

Each structural element is associated to a description of its lay-up of composite plies, together with the definition of their mechanical properties. When multiple plies are used, classical laminate analysis is used to derive the properties of the equivalent composite laminate from the properties of the individual plies.

Given the geometry of each airfoil, a two-dimensional finite element mesh is automatically generated for each section through a dedicated pre-processor, which employs a pivot technique to arrange the spatial density of the grid elements (see Figure 2, at right). Given its spatial mesh, each cross section is analyzed with a finite element method based on the anisotropic

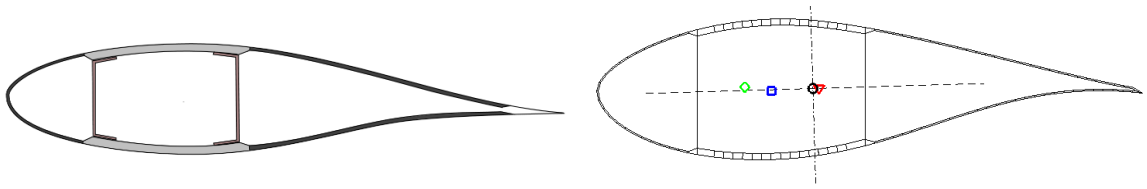

Figure 2. At left, three-cell blade section. At right, finite element mesh for the cross-sectional analysis, and relevant points.

beam theory developed in [18]. This yields the sectional mass and inertia properties, as well as a fully populated stiffness matrix which accounts for the couplings (e.g., flap-torsion, flap-lag) induced by the use of composite anisotropic materials. The output of this analysis includes also the location of centroid, elastic and shear centers, as well as the orientation of the principal axes. By this procedure, one may compute all necessary sectional properties whenever a blade section is modified by the design algorithm, because of changes in the aerodynamics and/or the structural variables.

The same finite element formulation furnishes recovery relationships that yield the sectional state of deformation and stress under a given set of sectional resultants. To perform the verification of the blade ultimate loading conditions, the wind turbine is simulated in a storm while the rotor is idling, for different wind directions and intensities; in a more complete and realistic setting, additional DLCs should be considered to define the load envelope [2, 3]. The resulting peak internal force and moment resultants are computed at each section of interest, and the associated stresses and strains are readily computed by recovery relationships [18]. Such conditions enter then into the definition of the design constraints (4).

Similarly, after linearization, the blade beam model readily yields the rotating frequencies of the blade, which are then used for the evaluation of the frequency placement constraints (3).

4. Applications and results

In the following, we investigate the capabilities of the free-form approach through the optimization of a 45-meter rotor blade, equipping a three-bladed upwind variable-speed wind turbine. The machine has a rated power of 2 MW, a rotor radius of 46.2 m, a cone angle of 1.0 deg, and cut in and cut out speeds of 3 and 25 m/s, respectively.

A non-dimensional coordinate η has origin at the root ($\eta = 0$) and terminates at the blade tip ($\eta = 1$), running parallel to the pitch axis. Both chord and twist are described by a fifth order Bézier curve and its six control points. The first control point at $\eta = 0$ is considered as frozen, to avoid changes to the radius of the cylindrical section at the blade root. The last control point at $\eta = 1$ is also constrained, in order to ensure a sufficient chord close to the tip to accommodate the end of the shear webs. The initial blade is equipped with two cylindrical sections and a family of five symmetric airfoils, named TEST-XX-S, where XX stands for the percent thickness and S stands for symmetric. Such choice of airfoils was made to investigate the capability of the proposed approach in finding solutions, even when starting from initial guesses that are far from the optimum. The position of each airfoil along the blade is shown in Table 1.

The structural layout of the blade is based on a three-cell section, with straight shear webs glued at the margins of the spar caps. Webs and caps are defined between $\eta = 0.1$ and $\eta = 0.978$, with the caps gradually tapering off past these two values. At the beginning of the process, the initial thickness of the various elements is defined along the blade and, while the thickness of the shell and of the webs is kept constant, the optimization is allowed to resize the spar cap thickness, discretized at 6 nodal stations along the blade and linearly interpolated in between

Number	Active	Airfoil	Thickness %	η
1	No	Cylinder	100	0
2	No	Cylinder	100	0.022
3	Yes	TEST-40-S	40	0.129
4	Yes	TEST-30-S	30	0.284
5	Yes	TEST-25-S	25	0.403
6	Yes	TEST-21-S	21	0.557
7	Yes	TEST-18-S	18	1

Table 1. Initial airfoils of the 2 MW wind turbine.

nodes. The blade is made with three different materials: a unidirectional carbon fiber is used in the spar caps, while biaxial and triaxial glass fiber for the shell and the shear webs, respectively.

Goal of the optimization is to minimize the CoE, while simultaneously satisfying all requirements, including the placement of the first flap frequency and conditions on maximum stresses in the structural elements. Since the design is conceived for onshore applications, the tip speed is constrained to 72 m/s in order to limit noise emissions. The AEP is computed using a Weibull with $V_{\text{ave}} = 10$ m/s. The results of this design optimization exercise are listed in Table 2.

	CoE [$/MWh]	AEP [MWh/yr]	C_P^* -	λ^* -	$V_{II1/2}$ [m/s]	V_r [m/s]	w_b [Kg]	f_{flap} [Hz]
Initial blade	49.9	7.54e03	0.423	8.31	8.90	10.49	7575	0.995
Optimal blade	46.9	8.09e03	0.487	6.91	9.75	10.00	7245	0.862

Table 2. Aero-structural optimization results for the 2 MW wind turbine.

The optimization achieves a significant improvement in the blade performance, with a 6.01 % reduction in the CoE. This is obtained by a simultaneous improvement of the aerodynamic design, with a 7.3 % increase in the AEP, as well as of the structural design, which results in a 4.36 % reduction in the total blade weight w_b. The maximum power coefficient C_P^* increases substantially, and its associated TSR λ^* decreases, in turn reducing the extent of the transition region. It must be noticed, however, that such dramatic improvements are largely due to the presence of symmetric airfoils on the initial blade, which was therefore very far from being optimal. The frequency constraint is active at convergence, while stress constraints are not.

Figure 3 shows the spanwise chord (at left) and twist (at right) shapes, before and after optimization. The primary effect of the design optimization is a reduction in the rotor solidity. This brings a substantial contribution in the reduction of the blade weight, which is an important component of the significant improvement observed in the CoE. This has also the effect of lowering peak loads, which in fact are not generating active constraints in the optimized blade. The twist seems to experience only minor variations from the initial configuration. This could be explained by considering that the twist is usually modified in order to adjust the local inflow angle so that a good value of the efficiency is achieved. In the free-form approach, however, the optimization can operate also on the airfoils, whereby the local lift and drag can be directly adjusted by working on the airfoil thickness and camber.

Figure 4 illustrates the design of three different airfoils, taken respectively close to the hub, at the mid-span and in proximity of the tip of the blade. It is evident that each airfoil has undergone relevant modifications in its final shape, as expected, given that the initial airfoils were symmetric. It is also interesting to observe the local adaption of the airfoil shapes.

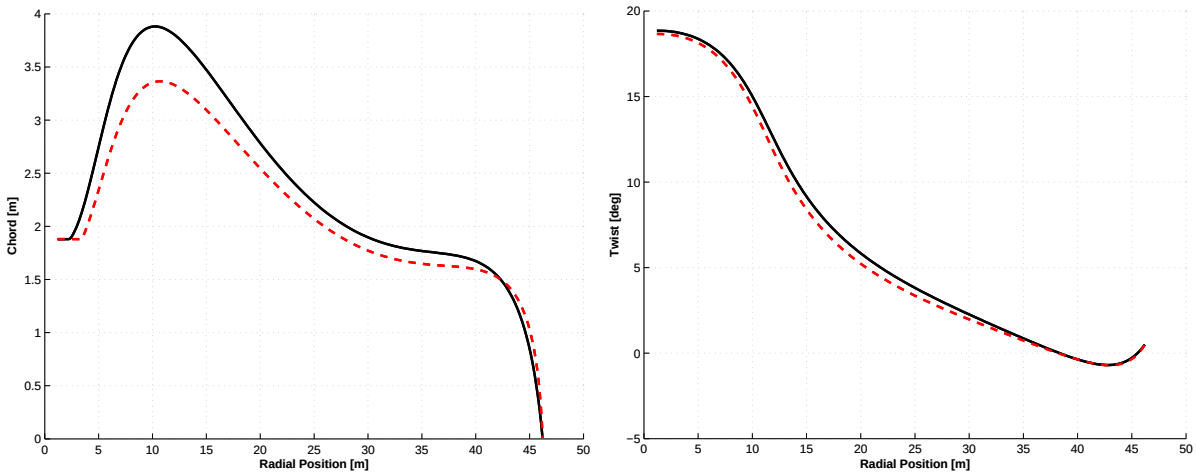

Figure 3. Chord (at left) and twist (at right) spanwise distributions for the 2 MW wind turbine. Initial configuration: black solid line; optimized configuration: dashed red line.

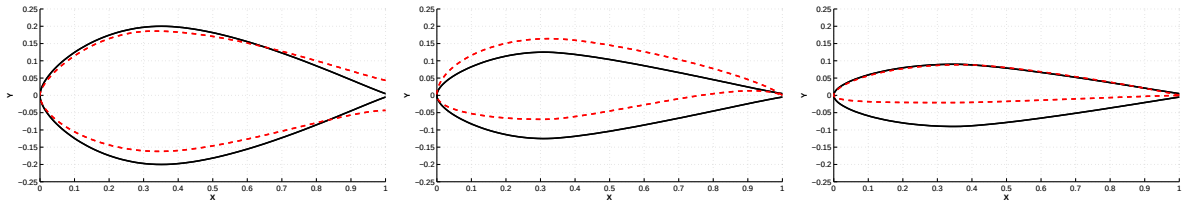

Figure 4. Initial and optimized airfoil shapes at three different spanwise stations for the 2 MW wind turbine. Initial configuration: black solid line; optimized configuration: dashed red line.

Starting from the hub region, the changes in the TEST-40-S airfoil seem to be driven primarily by structural considerations. In fact, some thickness appears at the trailing edge, which results in a flatback airfoil. As the sectional flap-wise stiffness is reduced by lowering the chord, the flatback shape compensates with a larger sectional inertia, thus helping in the enforcement of the frequency placement constraint. It must be noticed, however, that the final airfoil is characterized by a lower thickness than the initial one, which implies a slight enhancement of the aerodynamic efficiency. In fact, it appears that even small improvements in the aerodynamic characteristics of airfoils can have measurable implications on the AEP, even for the blade sections closer to the root.

The TEST-25-S airfoil also differs in a significant way from the initial symmetric shape. Specifically, the mean line of the airfoil has been modified in order to increase the camber, and thus the lift, so that the efficiency of the optimal airfoil is significantly higher than the initial one. This suggests that, moving from the hub-region towards the tip, the importance of the local aerodynamic performance of the blade increases while the structural aspects become less relevant, as expected according to intuition. The optimal shape shows a S-tail for rear loading on the pressure side [19].

For the TEST-18-S located at the blade tip, the optimization works essentially on the aerodynamic efficiency, which in this case is enhanced mainly by reducing the thickness of the airfoil rather than increasing lift. This confirms that the design of the tip region is driven by aerodynamic considerations, again according to intuition. The significant thickness reduction observed in the solution can be limited by using geometric constraints, which could result in a more lift-oriented design, but might also increase loads and hence bending moments.

5. Conclusions

In this work we have investigated a free-form approach for the aero-structural optimization of rotor blades. This method offers an improved optimization capability, allowing the simultaneous design of the blade and of its airfoils, thereby achieving a true three-dimensional optimization.

The analysis of the results allows to draw some conclusions:

- Although existence and uniqueness of the solution cannot be guaranteed in general, the procedure was always capable of delivering reasonable and convincing designs. In fact, even the rather radical choice of starting from symmetric airfoils was shown to work well.
- The optimal design of the various airfoils pursues different goals depending on the location of the airfoil along the blade. Specifically, airfoils close to the hub region appear to be driven by structural and stiffness considerations, while moving towards the tip a greater role of the aerodynamic effects can be observed. This behavior, which is actually quite typical and to be expected, was achieved naturally by the proposed approach, under the simple guide of the cost function and constraints.
- Some typical solutions adopted in large wind turbines emerged automatically during the design of the airfoils, as for example the presence of flatback airfoils near the hub and the appearance of the typical S-tail shape.

References

[1] Bottasso C L Croce A Sartori L and Grasso F 2013 Integration of airfoil design during the design of new blades *Proc. Int. Conf. on aerodynamics of offshore wind energy systems and wakes* Lyngby, Denmark June 17-19 p 327.
[2] *Guideline for the Certification of Wind Turbines* (Hamburg: Germanischer Lloyd Industrial Services GmbH)
[3] *Wind Turbines - Part 1: Design Requirements* (Hamburg: Germanischer Lloyd Industrial Services GmbH)
[4] Zhou J L Tits A and Lawrence C T 1997 *User's guide for FFSQP version 3.7* (University of Maryland)
[5] L. Fingersh Hand M and Laxson A 2006 *Wind turbine design cost and scaling model* (Golden: National Renewable Energy Laboratory) NREL/TP-500-40566
[6] Ning A Damiani R and Moriarty P 2013 Objectives and constraints for wind turbine optimization *51st AIAA Aerospace Sciences Meeting* Grapevine, USA January 7-10
[7] Bottasso C L Croce A and Campagnolo F 2012 Multi-disciplinary constrained optimization of wind turbines *Multibody Syst. Dyn.* **27** 21-53
[8] Bottasso C L Campagnolo F Croce A Dilli S Gualdoni F and Nielsen M B 2013 Structural optimization of wind turbine rotor blades by multi-level sectional/multibody/3D FEM analysis *Multibody Syst. Dyn. on-line*
[9] Grasso F 2013 Development of thick airfoils for wind turbines *J. Aircraft* **50** 975-81
[10] Piegl L and Tiller W, 1997 *The NURBS Book* (Springer-Verlag, Berlin and Heidelberg)
[11] Drela M 1989 *XFOIL: an analysis and design system for low reynolds number airfoils* (Cambridge: MIT Dept. of Aeronautics and Astronautics)
[12] Drela M 2001 *XFOIL 6.94 User guide* (Cambridge, USA: MIT Dept. of Aeronautics and Astronautics)
[13] Viterna L A and Corrigan R D 1981 *Fixed pitch rotor performance of large horizontal axis wind turbines* (NASA Scientific & technical information)
[14] Hansen M O L 2008 *Aerodynamics of Wind Turbines* (London, UK: Earthscan)
[15] Moriarty P J Hansen A C 2005 *AeroDyn theory manual* (Golden, USA: National Renewable Energy Laboratory) NREL/TP-500-36881
[16] Bottasso C L Croce A Riboldi C E D and Nam Y 2012 Power curve tracking in the presence of a tip speed constraint *Renew. Energ.* **40** 1-12
[17] Bir G 2005 *User's guide to BModes (Software for computing rotating beam coupled modes)* (Golden: National Renewable Energy Laboratory)
[18] Giavotto V Borri M Mantegazza P and Ghiringhelli G 1983 Anisotropic beam theory and applications *Comput. Struct.* **16** 403-13
[19] Bertagnolio F Sørensen N Johansen J and Fuglsang P 2001 *Wind turbine airfoil catalogue* (Roskilde: Risø National Laboratories) Risø-R-1280